Int. J. Electrochem. Sci., 13 **(2018)** 12331 – 12339, doi: 10.20964/2018.12.25

International Journal of ELECTROCHEMICAL SCIENCE
www.electrochemsci.org

Short Communication

Electromagnetic properties of nanocrystalline Mn-Zn ferrite synthesized from spent Zn-C battery via Egg-white route

Y.M. Al Angari

Chemistry department, Faculty of Science, King Abdulaziz University, Jeddah, KSA
E-mail: mam_999@yahoo.com

Received: 27 June 2018 / *Accepted:* 13 September 2018 / *Published:* 5 November 2018

Nanocrystalline $Mn_{0.8}Zn_{0.2}Fe_2O_4$ was successfully synthesized via egg-white auto-combustion route using waste Zn-C batteries as raw materials. The objective of this recycling process is to turn the contents of these waste batteries into valuable magnetic products, which realizes both environmental and economic benefits. Differential thermal analysis-thermogravimetry (DTA-TG) measurements were used to characterize the auto-combustion route and ferrite formation. X-ray diffraction (XRD), Fourier transform infrared (FT-IR), transmission electron microscopy (TEM) techniques were used to characterize the produced ferrite. The obtained weak magnetic properties measured via vibrating sample magnetometer (VSM) indicated the effect of the entire egg-white fuel on the combustion process and ferrite formation. Ac-conductivity measurements indicated semiconducting properties with transition at about 555 K attributed to change in the magnetic characterization from ferro- to paramagnetic one. The dielectric measurements as a function of frequency and temperature showed a gradual decrease with increasing frequency, which considered as a normal behavior of all ferrites.

Keywords: Mn-Zn ferrite, Egg-white, auto-combustion, ac-conductivity, dielectric.

1. INTRODUCTION

Manganese-zinc ferrites are ceramic soft magnetic material having mixed spinel structure in which Mn^{2+}, Zn^{2+} and Fe^{3+} ions are distributed throughout the tetrahedral and octahedral sites. This special structure enhances their magnetic permeability, saturation magnetization, dielectric resistivity and core losses [1-3]. Due to these excellent properties, they have been widely used in many electronic applications such as storage systems, transformers, recording heads, drug delivery and medical diagnostics [4,5].

For the preparation of these ferrites, many investigators have been employed a lot of various techniques aiming at the production of smaller size crystals having more diversity and higher performance. In this category, many wet chemical methods have been developed including:

coprecipitation [6], hydrothermal [7], auto-combustion [8] and microemulsion [9]. Among these methods, the auto-combustion was found to overcome different limitations arising from using other methods due to its cheap, simple, fast and energy saving. In literature, many fuels were successfully utilized in the auto-combustion reactions for the effective synthesis with modified properties such as glycine, urea, citrate and gelatin [10-13]. As a new route, Egg-white was recently employed as a fuel for the auto-combustion formation of many ferrites [14,15].

In the recent years, more and more zinc-carbon (Zn-C) dry batteries are used as power sources for many electric appliances. After short lifespan, same amount are discarded as wastes. The main components of these spent dry batteries are metallic zinc, manganese oxides and carbon. Hence, the recovering of these metallic wastes as Mn-Zn ferrites will effectively utilize these spent batteries as secondary metallic resources as well as solve many environmental pollution problems caused by their abandoning.

In literature, many investigations are adopted for recycling Zn-C batteries into valuable Mn-Zn ferrites. Kim [16] recovered Mn–Zn ferrite from spent Zn-C batteries via reductive acid leaching followed by oxidative precipitation processes. Gabal [13-15,17] prepared $Mn_{1-x}Zn_xFe_2O_4$ ($0.2 \leq x \leq 0.8$) nano-crystalline ferrites through reductive acid leaching of Zn-C batteries followed by different auto-combustion processes using citrate, urea, gelatin and sucrose as fuels. In all cases, the synthesizing process affected the different properties as well as the performances of the obtained Mn-Zn ferrites.

The main purpose of this manuscript is to recover spent Zn-C batteries into valuable Mn-Zn ferrite via reductive acid leaching followed by auto-combustion process utilizing environmental friendly egg-white precursor as fuel. The structural, morphology, electrical and magnetic properties of the obtained ferrite will be characterized using XRD, FT-IR, TEM, VSM ac-conductivity and dielectric measurements.

2. EXPERIMENTAL

$Mn_{0.8}Zn_{0.2}Fe_2O_4$ nano-crystalline ferrites was prepared through a multi-step process including: acid leaching, chemical treatment of Zn-C dry batteries waste and Egg-white precursor auto-combustion route. Firstly, the spent Zn-C dry batteries raw materials were dismantled, crushed, washed with distilled water and dried. The residues were leached in 2 mol L^{-1} nitric acid containing 2 wt % hydrogen peroxide under vigorous stirring at 60^{o}C. After complete dissolution, the resultant solution was filtered and the filtrate components were analyzed using atomic absorption spectroscopy as in our previous work [11].

Secondly, to prepare the entire ferrite, stoichiometric ratios of pure manganese nitrate, zinc nitrate and iron nitrate (BDH) were added to the filtrate in order to adjust Mn, Zn and Fe concentrations to the proper ratios. The Egg-white solution (60 ml Egg-white and 40 ml distilled water) was then added under vigorous stirring at room temperature. The formed gel precursor was digested and evaporated at about 80^{o}C till dryness. By rising the temperature, the obtained powder was auto-combusted with the evolution of gases and formation of fluffy solid powder. This powder was

given the name; as-prepared precursor and stored in a desiccator. A part of this powder was further ignited in an electrical oven at 500^{o}C for 1 h and kept in desiccator.

The structure and phase identification were performed using XRD Bruker axs D8 with Cu-Kα radiation (λ = 0.15418 nm) and FT-IR, Perkin–Elmer in the range of 800–200 cm^{-1} using KBr-pellet technique. The particle size and morphology were characterized using a JEOL 2010 TEM (100 kV). The auto-combustion reaction was followed through differential thermal analysis-thermogravimetry (DTA-TG) measurements in air using Perkin Elmer thermal analyzer. The magnetic properties were measured using a vibrating sample magnetometer (VSM-9600M) at R.T. up to applied magnetic field of 15 kOe. The ac-conductivity as well as the dielectric properties were measured as a function of temperature (up to 700 K) and frequency (100 Hz - 5 MHz) using a Hioki LCR bridge model 3531 and two probe method.

3. RESULTS AND DISCUSSION

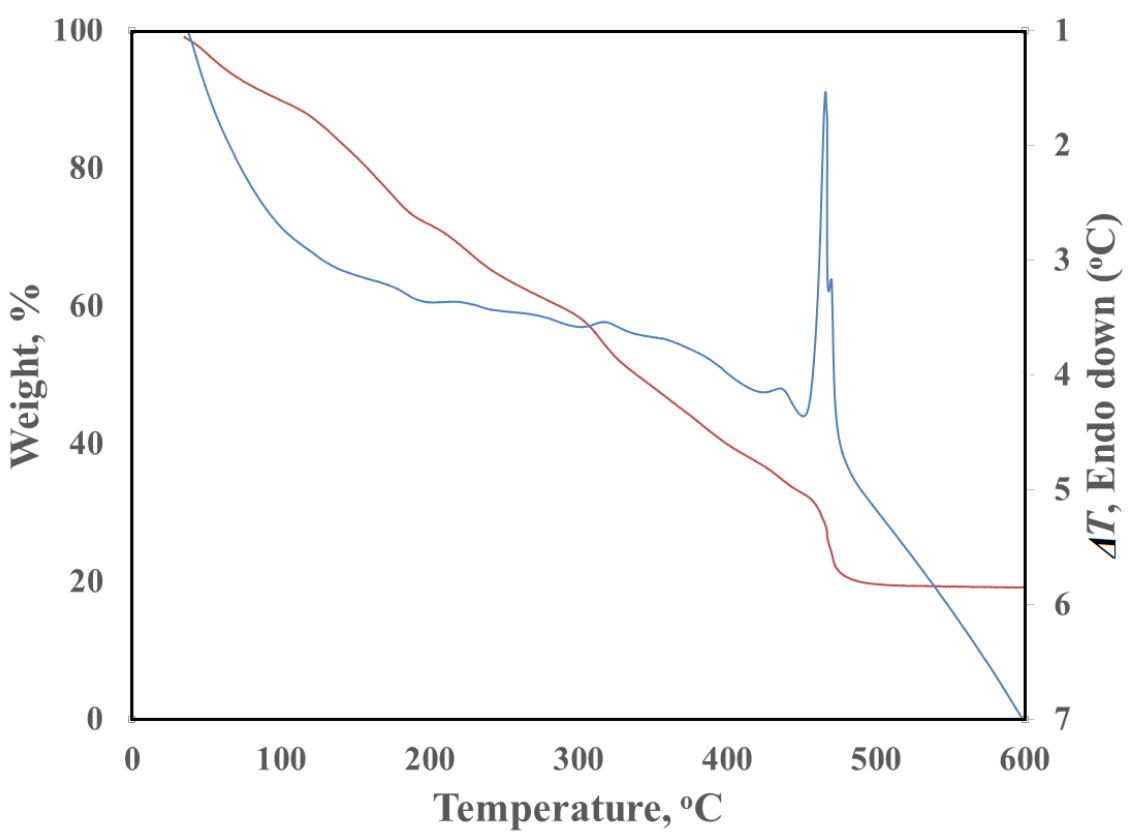

Figure 1. DTA-TG curves of gel-precursor in air. Heating rate = 5^{o}C min^{-1}.

The thermal decomposition behavior (DTA-TG) of the gel precursor (Fig. 1) displayed that, the decomposition begins with the release of hydrated water through many successive TG steps. The very broad endothermic DTA peak in the range 25-180^{o}C besides others smaller successive ones are characterizing this process. The exothermic nature of the last TG step in the range 455-480^{o}C suggested the oxidative decomposition of the nitrate as well as the Egg-white organic moiety of the

precursor. The absence of any weight loss or thermal changes behind 500°C confirmed the completion of the decomposition process and suggested the ferrite formation in agreement with the chosen calcination temperature (500°C) of the entire precursor.

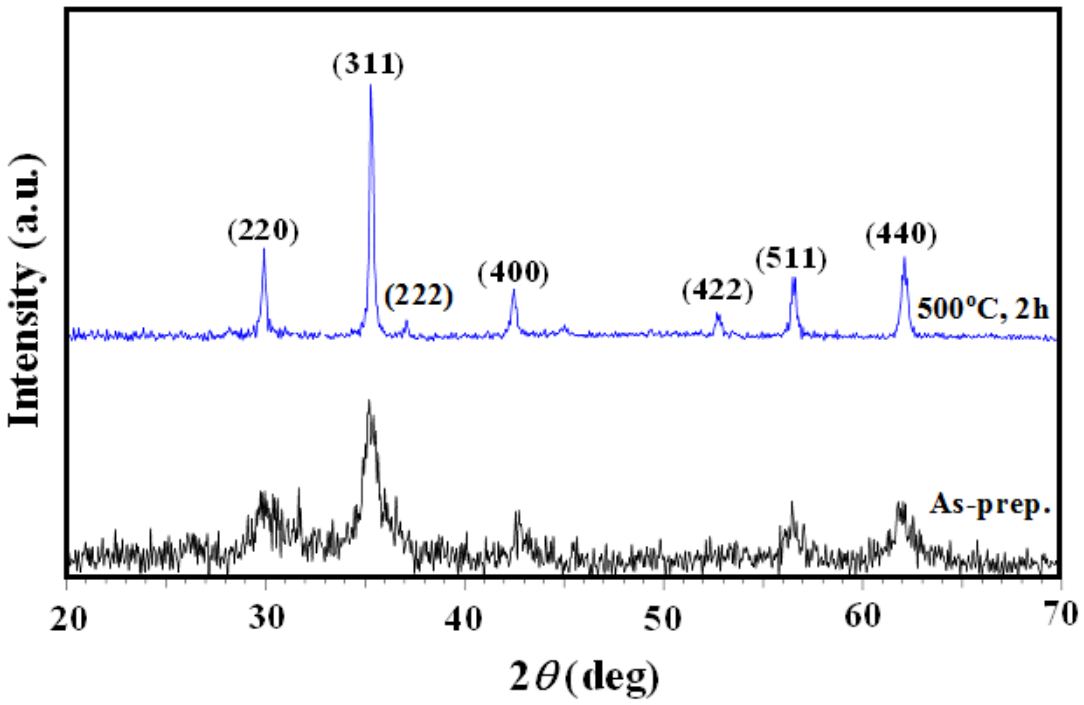

Figure 2. XRD patterns of as-prepared precursor and precursor calcined at 500°C.

Figure 2 exhibited XRD pattern of the as-prepared Egg-white precursor and precursor calcined at 500°C. The pattern of the as-prepared precursor showed the formation of the entire ferrite with very low crystallinity. After calcining at 500°C, the crystallinity improvement without any indication for the presence of any detectable impurity traces, suggested the formation of single-phase crystalline ferrite with reflections: (111), (220), (311), (222), (400), (422), (511) and (440) in agreement with JCPDS file No.: 74-2399 corresponding to $MnFe_2O_4$.

FT-IR spectra of the calcined precursor (Fig. 3a) showed the characteristic ferrite bands at 543 and 375 cm^{-1} attributed to the intrinsic stretching vibrations of the metal-oxygen at the tetrahedral and octahedral sites, respectively [18].

TEM image of the calcined precursor (Fig. 3b) exhibited well crystalline cubic nanoparticles with average particle size of about 15 nm. The particles agglomeration could be attributed to the experience of a permanent magnetic moment proportional to the particles volume [19].

Hysteresis loop of the calcined precursor (Fig. 3c) indicated weak ferromagnetic characteristic with saturation magnetization and coercivity amounted to 15.9 emu/g and 65.5 Oe, respectively. The non-saturation magnetization observed indicated the presence of antiferromagnetic interactions accompanying the ferromagnetic ones inside the clusters [20].

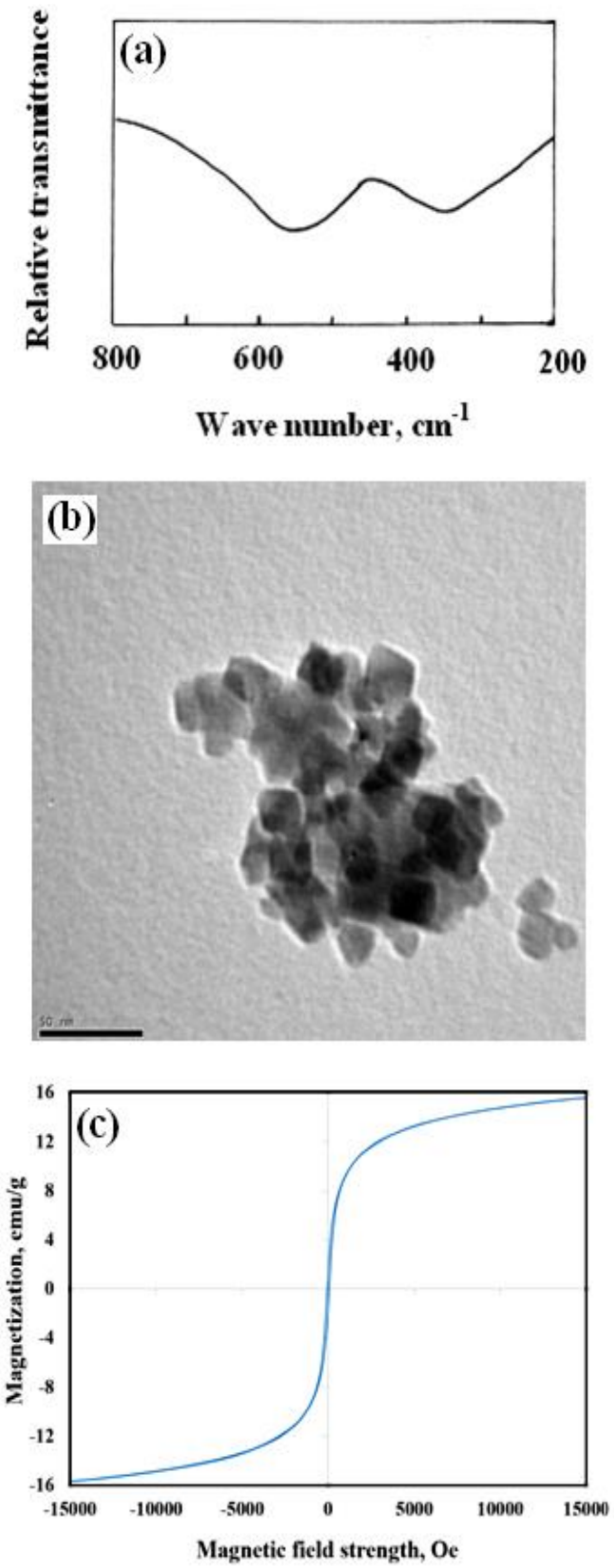

Figure 3. (a) FT-IR spectra, (b) TEM image and (c) Hysteresis loop of precursor calcined at 500^{o}C.

Table 1 indicated that this obtained magnetization appeared to be much lower than that reported for Mn0.8Zn0.2O4 ferrite prepared via solid-state [21] and auto-combustion routes [22,23].. At the same time, on comparison with our previous works on Mn0.8Zn0.2Fe2O4 nano-crystalline ferrites prepared using spent Zn-C batteries and different fuels including; gelatin [11], urea [12] and citrate [13], the entire magnetization value still indicated lower value. This exhibited the great impact of the entire used fuel on the obtained magnetic properties and suggested different applications.

Table 1. Magnetization values in comparison with others reported in literature.

(M_s)	(H_c)	Ref.
32.9	94.2	11
51.5	56.9	12
36.5	34.9	13
59.1	17.6	21
62.0	80.0	22
56.23	0.01	23
15.9	65.5	Present

Fig. 4 illustrated the electrical properties behavior viz.; ac-conductivity and dielectric constants (ε`and ε``) as a function of temperature and frequency. The ac-conductivity vs. temperature as a function of frequency showed three different regions. In the first one, the decreasing behavior by increasing temperature could be assigned to the loss of water content (mainly adsorbed on the ferrite surface). This water content is acting as electrons source and its evaporation decrease the number of charge carriers and conductivity. Similar behavior is reported by Gabal [24] for cobalt ferrite prepared via sucrose assisted combustion route.

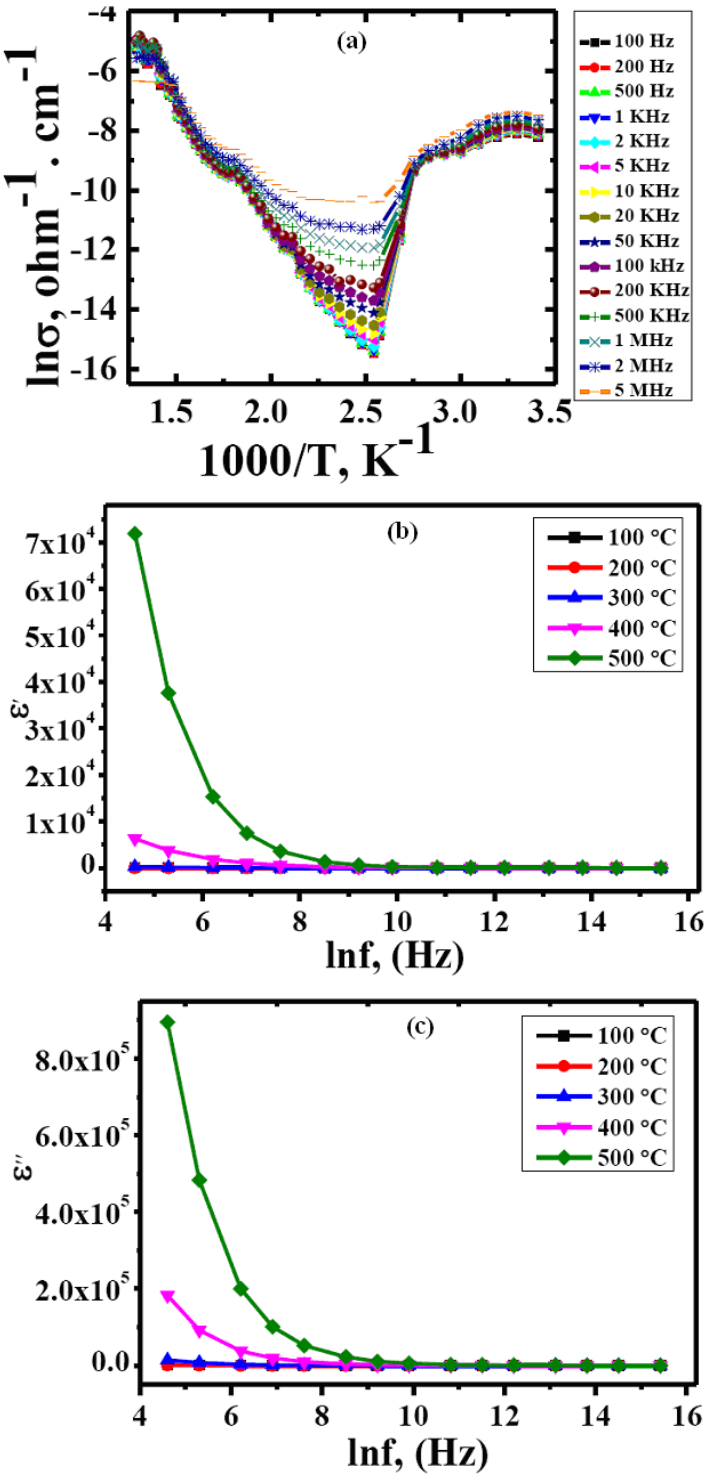

Figure 4. (a) lnσ vs. reciprocal of absolute temperature, (b) Real part of dielectric constant (ε`) vs. applied frequency as a function of temperature and (c) Imaginary part of dielectric constant (ε``) vs. applied frequency as a function of temperature.

In the following two regions, the conductivity vs. reciprocal temperature exhibited a gradual increase with increasing temperature (obeying Arrhenius relation) indicated semi-conducting behavior. This obvious increase in conductivity may be attributed to the increase in mobility of the charge

carriers' as a result of increasing thermal energy. The change in the slope of the Arrhenius relation by increasing temperature could be attributed, in accordance with the previous studies [25,26] to the magnetic transition from ferro- to paramagnetic characteristics. The relatively lower obtained Curie temperature (T_c) at 555 K compared with those previously reported [25,26] indicated weak ferromagnetic properties.

From a closer look at Fig. 4a, the conductivities are appeared to be frequency dependent at the ferromagnetic region while frequency independent at paramagnetic region. This behavior suggests that the conduction in the low temperature range could be attributed to the electron hopping between different valence cations and changed to polaron conduction at higher temperature range [24]. This suggestion was also reinforced through the comparison of the activation energies calculated using Arrhenius relation for the two regions where the smaller slope of $\ln\sigma$ vs. temperature relation obtained at low temperature region results in lower activation energy suitable for the hopping conduction. On the other hand, the higher activation energy obtained at high temperature region is equivalent to the polaron conduction required higher thermal energy.

Fig.4b showed the frequency dependence of real (ε`) and imaginary (ε``) parts of dielectric constant as a function of temperature. From the figure, it is obvious that both values at all temperatures indicated descending behavior with increasing frequency till attains constant values at higher frequencies. This behavior is a general behavior of most ferrites and agreed well with the Maxwell-Wagner type interfacial polarization and Koop's phenomenological theory [27]. Generally, the polarization arises from the orientation of electrons produced from electron exchange occurred between Fe^{2+} and Fe^{3+} ions in the direction of the applied electrical field. Increasing frequency beyond a certain value results in electrons dispersions and polarization decrease since the electron exchange cannot follow the alternating electrical field. A similar behavior was reported by Iqbal et al for Mn-Zn ferrites prepared via coprecipitation method [28].

4. CONCLUSIONS

Magnetically soft Mn-Zn ferrite nanocrystalline having mean crystallite size of 15 nm were successfully prepared using spent Zn-C batteries as raw materials via multi-step processes including acid leaching, reduction and egg-white precursor auto-combustion. This simple, green and fast route proved its economic advantage in this recycling technology. XRD, FT-IR, TEM and VSM measurements assured single-phase ferrite formation. Ac-conductivity measurements indicated a magnetic transition from ferro- to paramagnetic by increasing temperature along with changing of the conduction mechanism from hopping to polaron one.

References

1. M. Sugimoto, *J. Am. Ceram. Soc.*, 82 (1999) 269.
2. A. Goldman, Modern ferrite technology, Marcel Dekker Inc., New York, 1993.
3. G. Ott, J. Wrba and R. Lucke, *J. Magn. Magn. Mater.*, 254–255 (2003) 535.
4. Z. Zheng, X. Zhong, Y. Zhang, H. Yu and D. Zeng, *J. Alloys Compd.*, 466 (2008) 377.

5. S. Dasgupta, K.B. Kim, J. Ellrich, J. Eckert and I. Manna, *J. Alloys Compd.*, 424 (2006) 13.
6. A. Angermann, E. Hartmann and J. Topfer, *J. Magn. Magn. Mater.*, 322 (2010) 3455.
7. Z. Klencsar, G. Tolnai, L. Korecz, I. Sajo, P. Nemeth, J. Osan, S. Meszaros and E. Kuzmann *Sol. State Sci.*, 24 (2013) 90.
8. K. Jalaiah and K.V. Babu,. *J. Magn. Magn Mater.*, 423 (2017) 275.
9. D.S. Mathew and R.S. Juang, *Chem. Eng. J.*, 129 (2007) 51.
10. A.C.F.M. Costa, V.J. Silva, C.C. Xin, D.A. Vieira, D.R. Cornejo and R.H.G.A. Kiminami, *J. Alloys Compd.*, 495 (2010) 503.
11. M.A. Gabal, R.S. Al-luhaibi and Y.M. Al Angari, *J. Hazard. Mater.*, 246–247 (2013) 227.
12. M.A. Gabal, R.S. Al-Luhaibi and Y.M. Al Angari, *J. Magn. Magn. Mater.*, 348 (2013) 107.
13. M.A. Gabal, R.S. Al-luhaibi and Y.M. Al Angari, *Powder Technol.*, 256 (2014) 32.
14. M.A. Gabal, Y.M. Al Angari and H.M. Zaki, *J. Magn. Magn. Mater.*, 363 (2014) 6.
15. M.A. Gabal, W.A. Bayoumy, A. Saeed and Y.M. Al Angari, *J. Mol. Stru.*, 1097 (2015) 45.
16. T.H. Kim, G. Senanayake, J.G. Kang, J.S. Sohn, K.I Rhee, S.W. Lee and S.M. Shin, *Hydrometallurgy*, 96 (2009) 154.
17. M.A. Gabal, E.A. Al-Harthy, Y.M. AlAngari, M. Abdel Salam and A.M. Asiri, *J. Magn. Magn. Mater.,*407 (2016)175.
18. R. D. Waldron, *Phys. Rev.*, 99 (1955)1727.
19. M.A. Gabal, *J.Magn. Magn, Mater.*, 321 (2009) 3144.
20. M.S. Tomar, S.P. Singh, O. Perales-Perez, R.P. Guzman, E. Calderon and C.R Ramos, *Microelectronics J.*, 36 (2005) 475.
21. M.M. Hessien, M.M. Rashad, K. El-Barawy and I.A. Ibrahim, *J. Magn. Magn. Mater.*, 320 (2008) 1615.
22. M. Syue, F. Wei, C. Chou and C. Fu, *Thin Film Sol.*, 519 (2001) 8303.
23. R. Gimenes, M.R. Baldissera, M.R.A. da Silva, D.A.W. Soares, L.A. Perazoli, M.R. da Silva and M.A. Zaghete, *Ceram. Int.*, 38 (2012) 741.
24. M.A. Gabal, A.A. Al-Juaid1, S.M. Al-Rashed, M.A. Hussein and F. Al-Marzouki, *J. Magn. Magn. Mater.*, 426 (2017) 670.
25. C. Rath, K.K. Sahu, S. Anand, S.K. Date, N.C. Mishra and R.P. Das, *J. Magn. Magn. Mater.*, 202 (1999) 77.
26. M.J.N. Isfahani, M. Myndyk, D Menzel, A. Feldhoff, J. Amighian and V. Sepelak, *J. Magn. Magn. Mater.*, 321 (2009) 152.
27. E. Melagiriyappa, H.S. Jayanna and B.K. Chougule, *Mater. Chem. Phys.*, 112 (2008) 68-73.
28. M.A. Iqbal, Misbah-ul-Islam, I. Ali, H.M. Khan, G. Mustafa and I. Ali, *Ceram. Int.*, 39 (2013) 1539.